INTERNATIONAL JOURNAL FOR NUMERICAL METHODS IN FLUIDS, VOL. 6, 895–911 (1986)

DEVELOPMENT OF NEW TRIANGULAR ELEMENTS FOR FREE SURFACE FLOWS

GOURI DHATT, AZZEDDINE SOULAIMANI

Civil Engineering Department, Laval University, Québec, Canada, G1K 7P4

YVON OUELLET

Director of Centre de Recherche sur les Applications Numériques en Ingénierie (CRANI), Québec, G1K 7P4, Canada

AND

MICHEL FORTIN

Department of Mathematics, Laval University, Québec, Canada, G1K 7P4

SUMMARY

New finite elements have been developed to simulate steady and unsteady two-dimensional free surface flows. The depth-averaged velocity components with the free surface elevation have been used as independent variables in the model. The differences between the various elements presented lie in the choice of velocity approximation. The Newton–Raphson method has been used to solve the non-linear system of equations. Emphasis is put on bench-mark examples to assess the accuracy and efficiency of the elements. A simple stable new element tested herein shows promising advantages for industrial finite element codes.

KEY WORDS Free Surface Flow Mixed Finite Elements Choice of Velocity Approximation

INTRODUCTION

For studying shallow water flows, Pritchard[1] has discussed various aspects of the depth-averaged two-dimensional model leading to average velocities (u, v) and variation of water level (h) as variables. Leenderste[2] and his group have used finite difference techniques to study estuary and river flows based on a similar model. The development of finite elements along with fast computing facilities attracted the attention of researchers in the early seventies to apply those techniques for analysing such flows. Taylor and Hood[3] used quadrilateral elements for studying two-dimensional flows with continuous biquadratic velocities and linear water level approximation, whereas Connor and Wang[4] tried simple triangular elements, with linear approximation for velocity and water level. In those early finite element works, numerical oscillations were observed in water level values which in certain cases had an influence on the whole velocity field. This was especially the case when linear triangular elements were used for studying closed estuary and steady large river flows. The work of Taylor and his colleagues concluded that the problem of oscillations can be solved by a proper choice of approximations for velocities and water levels. A heuristic recommendation was that the water level approximations should be one degree lower than the velocity approximations. In the meantime, the works of Brezzi[5] and Babuska[6] for mixed finite element models have led to the definition of consistency conditions (known as B.B.

0271–2091/86/120895–17$08.50

Received 5 December 1985
Revised 22 April 1986

or inf–sup conditions) for Stokes flows in order to obtain a solution without parasitic oscillations. There is now a large amount of literature published on this subject and we may mention among others, the works of Sani *et al.*,[7] Fortin,[8] Oden and Carey[9] and Girault and Raviart.[10] However, this analysis cannot be directly applied to free surface estuary flows. It is generally accepted that if a finite element approximation does not respect the inf–sup condition for Stokes flows, it will most probably give parasitic oscillations for free surface flows. Finite element models are at present successfully used to solve two-dimensional steady and unsteady flows. Cochet[11] and Cochet *et al.*[12] have made an elaborate study of various types of C^0 elements (u, v, h are continuous) in order to determine their efficiency for such flows. Based on different works, Walters and Cheng[13] have concluded that the quadrilateral element Q 9-4 (9 nodes for velocities, 4 corner nodes for elevations) and the triangular element T6-3 (6 nodes for velocities, 3 corner nodes for elevations) lead to solutions free of oscillations for different types of complex flows. Similar conclusions have been made for studying Stokes flows with such elements.

In the present study, we propose four new triangular elements, T6B, T3B, T6BN and T6N, for studying depth-averaged steady and unsteady flows. The water level h varies linearly and the velocity approximations are complete or incomplete quadratic with or without a bubble function. The development of these elements has been inspired by works of Fortin[8] on penalty elements for Stokes problems where the pressure approximation is discontinuous and Arnold *et al.*[14] on equal interpolation continuous pressure–velocity elements. Herein, we study different types of typical flows to evaluate the relative efficiency and accuracy of these elements.

MATHEMATICAL MODEL

The classical shallow water equations governing free surface flows are defined as follows:[1,2,11,15]

$$\frac{\partial u}{\partial t}+u\frac{\partial u}{\partial x}+v\frac{\partial u}{\partial y}-\frac{\partial}{\partial x}\nu\frac{\partial u}{\partial x}-\frac{\partial}{\partial y}\nu\frac{\partial u}{\partial y}+g\frac{\partial h}{\partial x}+\frac{gu}{C^2(H+h)}\sqrt{(u^2+v^2)}=F_x, \tag{1}$$

$$\frac{\partial v}{\partial t}+u\frac{\partial v}{\partial x}+v\frac{\partial v}{\partial y}-\frac{\partial}{\partial x}\nu\frac{\partial v}{\partial x}-\frac{\partial}{\partial y}\nu\frac{\partial v}{\partial y}+g\frac{\partial h}{\partial y}+\frac{gv}{C^2(H+h)}\sqrt{(u^2+v^2)}=F_y, \tag{2}$$

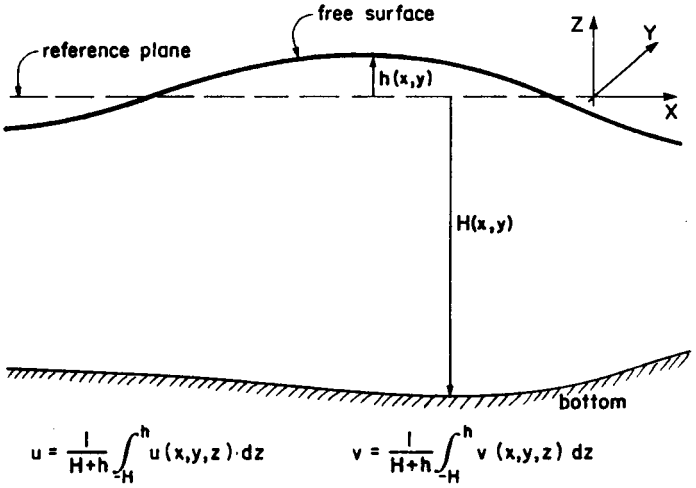

Figure 1. Definition sketch for shallow water free surface flow

$$\frac{\partial h}{\partial t}+\frac{\partial (H+h)u}{\partial x}+\frac{\partial (H+h)v}{\partial y}=0, \tag{3}$$

where u and v are the averaged velocity components and h is the surface level variation. We denote by H the depth of the bottom with respect to a reference plane (Figure 1). F_x and F_y are the external force components (e.g. forces due to wind). ν is introduced to include turbulence and numerical viscosity. This may depend on velocity or its gradient and a relevant mixing length choice. C is Chezy's coefficient to represent the bed rugosity; V denotes the fluid domain and S its boundary.

It is worth noting that the shallow water equations (1)–(3) are based on a hydrostatic pressure approximation and are thus limited to flows with small water surface and bed slopes.

WEAK VARIATIONAL FORMULATION

The weak formulation underlying our finite element scheme is a standard Galerkin model. Multiplying equations (1)–(3) by arbitrary test functions δu, δv, δh we thus want to find u, v and h such that

$$\begin{aligned} W=&\int_V \delta u\left(\frac{\partial u}{\partial t}+u\frac{\partial u}{\partial x}+v\frac{\partial u}{\partial y}+\frac{g\sqrt{(u^2+v^2)}}{C^2(H+h)}u+g\frac{\partial h}{\partial x}-Fx\right)\mathrm{d}V\\ &+\int_V \delta v\left(\frac{\partial v}{\partial t}+u\frac{\partial v}{\partial x}+v\frac{\partial v}{\partial y}+\frac{g\sqrt{(u^2+v^2)}}{C^2(H+h)}v+g\frac{\partial h}{\partial y}-Fy\right)\mathrm{d}V\\ &+\int_V \delta h\left(\frac{\partial h}{\partial t}+\frac{\partial (H+h)u}{\partial x}+\frac{\partial (H+h)v}{\partial y}\right)\mathrm{d}V\\ &+\int_V \nu\left(\frac{\partial \delta u}{\partial x}\frac{\partial u}{\partial x}+\frac{\partial \delta u}{\partial y}\frac{\partial u}{\partial y}+\frac{\partial \delta v}{\partial x}\frac{\partial v}{\partial x}+\frac{\partial \delta v}{\partial y}\frac{\partial v}{\partial y}\right)\mathrm{d}V\\ &-\int_S \nu\left(\delta u\frac{\partial u}{\partial n}+\delta v\frac{\partial v}{\partial n}\right)\mathrm{d}S=0. \end{aligned} \tag{4}$$

δu, δv and δh are the weighting functions belonging to the same functional spaces as u, v and h, respectively. In the finite element model C^0-type approximations for $(u,\delta u)$, $(v,\delta v)$ and $(h,\delta h)$ are used.

Many variants are possible for the above weak formulation. For instance the term $\int_V \delta\mathbf{u}\,\mathrm{grad}\,h\,\mathrm{d}V$ can be integrated by parts to yield $\int_V h\,\mathrm{div}\,\delta\mathbf{u}\,\mathrm{d}x$, and one can obtain $\int_V \mathrm{grad}\,(\delta h)\cdot(H+h)\mathbf{u}\,\mathrm{d}x+\int_S \delta h(H+h)\mathbf{u}\cdot\mathbf{n}\,\mathrm{d}s$, for the δh part ($\mathbf{n}$ denotes the outward normal direction to the boundary).

The choice of the formulation may change not only the choice of approximations but also natural boundary conditions, that is conditions hidden in the variational formulation itself. Care must be taken to use the correct form relative to the desired boundary conditions.

For natural flows, we encounter two types of boundary conditions:

1. For solid boundaries, it is a common practice in engineering applications to use free-slip or quasi-slip conditions to include boundary drag. At a point on the boundary, the velocity component is imposed to be zero along the normal direction. A tangential force law is defined to include the boundary layer drag effect along the tangential direction. In general, this force is assumed negligible as compared to the bottom friction force. For numerical

purposes the free-slip condition avoids oscillations and leads to savings in computational effort, since the relatively small boundary layer is neglected.

2. For open boundaries, the choice of boundary conditions depends on the availability of measured data. Very often, one imposes the water levels along with a chosen orientation of velocity. In certain fortunate situations, it is possible to use the velocity profiles.

PRESENTATION OF THE ELEMENTS

Straight edges are used to define the triangular geometry of elements. Approximations for water level and velocity components are represented on a reference element (Figure 2).

All the elements use the standard C^0 linear approximation for h and δh. However the difference lies in the choice of velocity approximations for each element.

T3B element (the mini-element)

This is the simplest triangular element satisfying the inf–sup condition.[14–16] It is identical to the element used by Connor and Wang but enriched by two internal degrees of freedom, representing velocity components. Each degree is associated with a bubble function ($\lambda_1, \lambda_2, \lambda_3$ in barycentric co-ordinates) which vanishes on the boundary of the element.

T6 element

This is the classical element employed by a large number of researchers[11,13,15,17] in fluid flow studies. The standard 6 term quadratic approximations are used to represent the fields of each velocity component. A proof of its stability for Stokes flows was given by Bercovier and Pironneau.[17]

T6B element

This differs from the T6 element by two additional internal degrees of freedom associated with the same bubble functions as in the T3B element. It is expected that this should improve the accuracy.

T6BN element

The development of this element is based on the technique first introduced by Fortin[8] and later used by Fortin[16] and Soulaimani.[15] This element is nothing but the T3B element with a

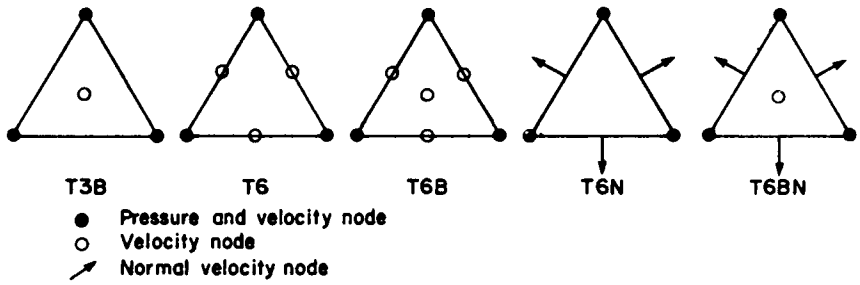

Figure 2. Presentation of the elements

Table I. Presentation of the elements

Symbol	Velocity approximation	Number of d.o.f.	d.o.f. after condensation	Stability
T3B	Linear for u and v plus internal bubble	11	9	Yes
T6	Quadratic for u and v	15	15	Yes
T6B	Quadratic for u and v plus internal bubble	17	15	Yes
T6BN	Quadratic for the normal component and linear for tangential, plus internal bubble	14	12	Yes
T6N	Identical to T6BN but without bubble	11	11	No

normal velocity component at each of the 3 mid-side points. Along each side, the normal velocity is quadratic, whereas the tangential one is linear. In practice, this element is built by post-processing the elementary matrix of the T6B element to eliminate the tangential points on the sides.[18]

T6N element

This is obtained by ignoring the internal degrees of freedom of the T6BN element. This element does not satisfy the inf–sup condition, but has nevertheless given, in some applications, acceptable results for velocities.

With respect to computational effort, T6, T6B, T6BN and T6N are comparable as to the construction of the matrix. A seven-point Gaussian integration scheme has been used. The T3B element can be integrated exactly, which leads to substantial savings. The solution cost is in direct relation to the number of degrees of freedom. Overall computing with T3B requires about 48 per cent of the effort needed with T6.

DISCRETIZED MODEL AND STRATEGY OF RESOLUTION

The discretized formulation (4) is equivalent to solving an algebraic non-linear system of equations defined as follows.

$$\mathbf{M}\{\dot{\mathbf{U}}\} + [\mathbf{K}(\{\mathbf{U}\})]\{\mathbf{U}\} = \{\mathbf{F}\}, \tag{5}$$

where $\{\mathbf{U}\}$ is the vector of all degrees of freedom and $\{\dot{\mathbf{U}}\}$ is its temporal derivative, $\mathbf{M}$ is the mass matrix and $\mathbf{K}$ is the rigid non-linear matrix.

We have used an implicit Euler scheme coupled with the standard Newton–Raphson method to solve the above system of equations.[19] It is worth noting here that the inclusion of all non-linear terms in the computation of the tangent matrix increases the convergence of the iterative process as demonstrated numerically in Reference 15. Indeed, the terms representing bottom shears are important and may dominate in shallow-water flows. Since they are non-linear with respect to velocity and free surface level, their derivatives should be included in the tangent matrix in order to achieve the quadratic convergence rate of the Newton–Raphson method. The solution strategy requires proper choice of step size and initial conditions, and an incremental introduction of velocity and water level boundary conditions.

Other time-stepping procedures could evidently be used. It could for example be advantageous to use a trapezoidal integration rule to obtain a second-order scheme. More stable schemes, such as Gear's, could also be thought of and future developments should include such features.

NUMERICAL EXAMPLES

The following bench-mark examples have been studied in order to test the efficiency and the stability of the elements presented in the previous section:

(a) simple steady flow with free surface
(b) complete two-dimensional free surface flow
(c) one-dimensional unsteady flow with different slopes.

The study is concluded with a practical example of flow analysis in the St. Lawrence River.

Steady free surface flow

We have studied a simple steady free surface flow where the non-linear terms in equations (1) and (2) have been neglected. The introduction of explicit external forces in a totally artificial situation permits working with a known exact solution. Thus the accuracy of the finite elements schemes could be easily tested.

It should be said that even in the simple case where $H = 0$ the equations are more intricate than a Stokes flow. The continuity equation (3) remains non-linear. A comparative study of the behaviour of the various elements, cited above, in the case of Stokes flows has been presented by Fortin *et al.*[20]

A square domain defined by $0 \leqslant x \leqslant 100$ and $0 \leqslant y \leqslant 100$ has been partitioned into regular triangular elements with various mesh sizes h (Figure 3).

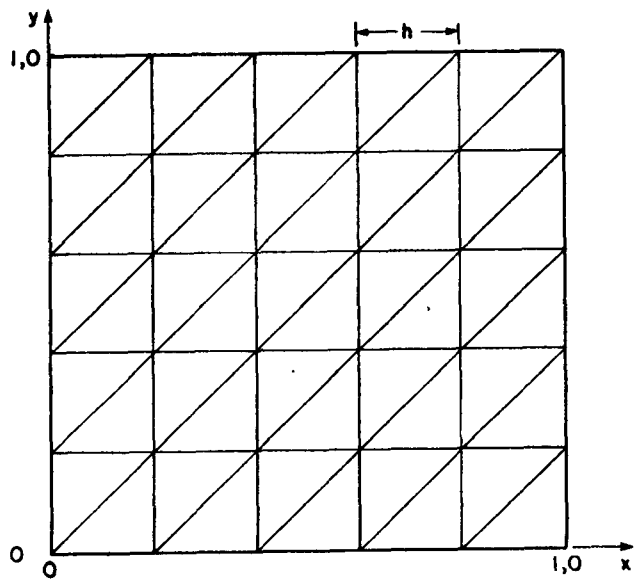

Figure 3. Example of regular space discretization. Boundary conditions: exact velocity imposed at all sides; exact water level imposed at one node. h = mesh size

The depth of the bottom is given by

$$H = 10 + \alpha(x + y), \quad \text{with } \alpha = 10^{-3}.$$

The external component forces are

$$F_x = \alpha^2(\alpha - 6y) \quad \text{and} \quad F_y = \alpha^2(\alpha - 6x).$$

The exact solution is then

$$u_{ex} = \alpha^2 y^3, \quad v_{ex} = \alpha^2 x^3 \quad \text{and} \quad h_{ex} = -\alpha(x + y).$$

Errors between the exact ($\mathbf{u}_{ex}$) and numerical solutions ($\mathbf{u}_h$) are evaluated by means of norms:

$$E_v = \|\mathbf{u}_h - \mathbf{u}_{ex}\|_1 \quad \text{and} \quad E_p = \|h - h_{ex}\|_0,$$

with

$$\|\mathbf{v}\|_1 = \int_V (\text{grad } \mathbf{v})^2 \, dV \quad \text{and} \quad \|q\|_0 = \int_V q^2 \, dV.$$

Velocity values have been specified at the boundary and the water level has been imposed at only one point ($x = 0$, $y = 100$). The solution has been obtained with use of the Newton–Raphson method and the norm of convergence of the iterative process has been limited to

$$\frac{\|\{\Delta \mathbf{U}\}\|_0}{\|\{\mathbf{U}\}\|_0} = 10^{-4}.$$

Variations of E_v and E_p (E_p is plotted only for the T3B, T6BN and T6N elements since the numerical surface elevation for T6B and T6 elements practically coincides with the exact solution) with mesh size are presented in Figures 4 and 5, and these show that

(i) the T3B, T6N and T6BN elements provide very similar results for the velocity field
(ii) the T6B element presents velocity errors very slightly less than those for the T6 element
(iii) the T6N element presents important errors of the free surface level
(iv) for the T3B element, the numerical water level converges linearly without any oscillations but it is less accurate than for the T6BN element (and of course T6 or T6B).

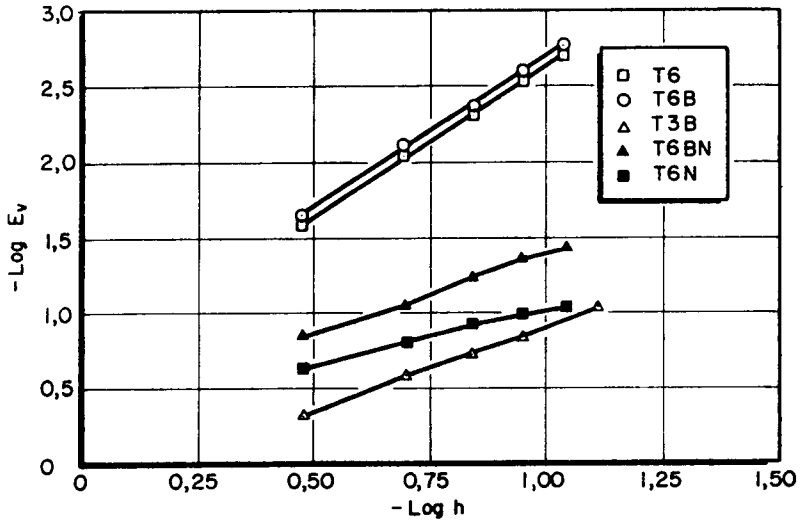

Figure 4. Variation of velocity error norm with mesh size

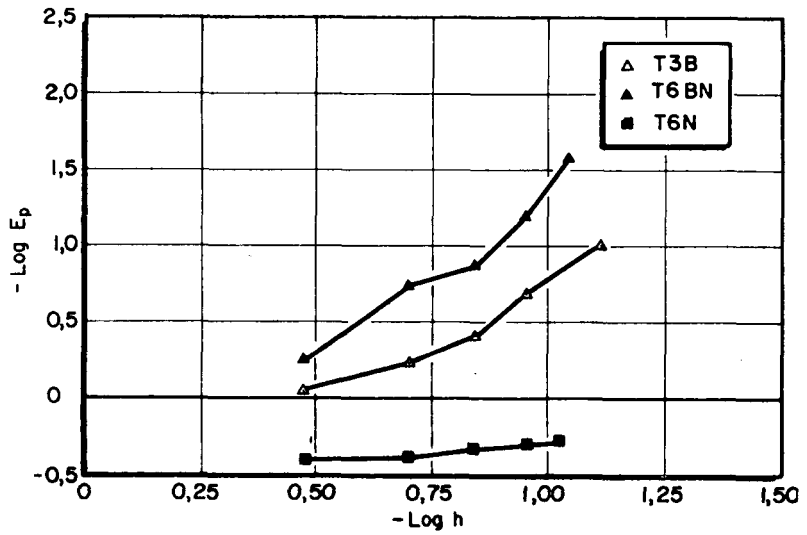

Figure 5. Variation of pressure error norm with mesh size (there is no error for T6 and T6B elements)

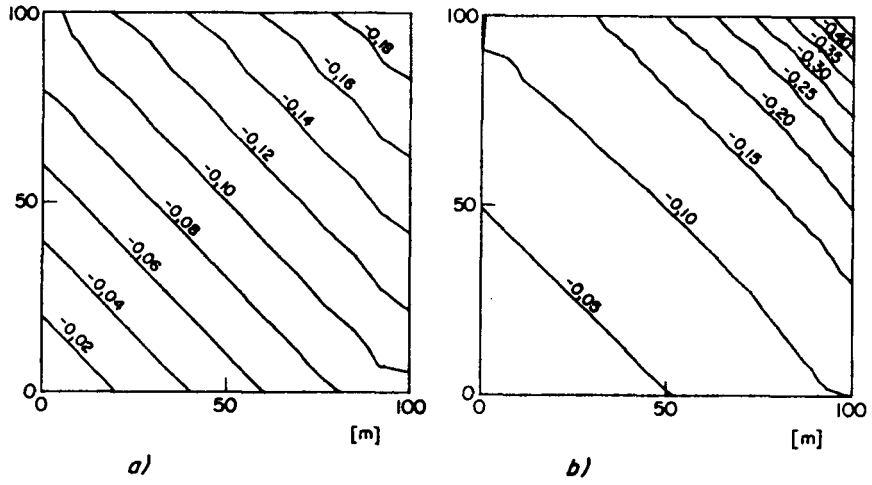

Figure 6. Free surface flow: isobars. (a) Element T3B. (b) Element T6N

Figures 6(a) and 6(b) show the isobars of the T3B and T6N elements. Figure 6(b) shows clearly that the computed water levels for the T6N element do not vary linearly, as expected from the exact solution and as computed by stable elements.

Bench-mark test: complete two-dimensional free-surface flow

We establish a bench-mark example to assess the quality of the various finite element schemes in a two-dimensional free surface flow where all non-linear terms are present. It consists of solving the set of equations (1)–(3) without any simplifications and of comparing the numerical results with the exact solution. The domain is defined by $0 \leqslant x \leqslant 100$, $0 \leqslant y \leqslant 100$, with

$H = 10 + \alpha(x + y)$ and $\alpha = 10^{-3}$. The hydraulics parameters are $v = 1{\cdot}0\,\mathrm{m^2/s}$, $g = 9{\cdot}81\,\mathrm{m/s^2}$, $C = 50{\cdot}0\,\mathrm{m^{1/2}/s}$ and the boundary conditions considered are as follows:

(a) exact values for velocities at all boundaries
(b) h specified at one point.

The external component forces are expressed by

$$F_x = -6\alpha^2 y + \alpha g + 3\alpha^4 x^3 y^2 + \frac{\alpha^4 g}{10C^2} y^3 \sqrt{(x^6 + y^6)},$$

$$F_y = -6\alpha^2 x + \alpha g + 3\alpha^4 x^2 y^3 + \frac{\alpha^4 g}{10C^2} x^3 \sqrt{(x^6 + y^6)},$$

for which the exact solution reads

$$u = \alpha^2 y^3,$$
$$v = \alpha^2 x^3,$$
$$h = -\alpha(x + y).$$

Tables II and III show numerical results observed at the first diagonal line of the domain for a mesh size equal to 0·2. This example confirms the above conclusions, that the T6 and T6BN

Table II. Comparison of the first diagonal surface levels: numerical results with exact solution for a two-dimensional free-surface flow

$\frac{x}{100} = \frac{y}{100}$	0	0·2	0·4	0·6	0·8	1	E_p
Exact	0	−0·04	−0·08	−0·12	−0·16	−0·20	
T3B	$-5{\cdot}0 \times 10^{-5}$	−0·04017	−0·08014	−0·12096	−0·16269	−0·20317	0·12704
T6	$8{\cdot}0 \times 10^{-6}$	−0·03999	−0·07999	−0·12006	−0·16021	−0·2009	0·015794
T6B	$-1{\cdot}0 \times 10^{-4}$	−0·0401	−0·0801	−0·1202	−0·16045	−0·20097	0·023236
T6BN	$-7{\cdot}6 \times 10^{-4}$	−0·04057	−0·08065	−0·12042	−0·16067	−·19908	0·049445
T6N	$-1{\cdot}3 \times 10^{-3}$	−0·041196	−0·081668	−0·12032	−0·16234	−0·1983	0·11659

Table III. Comparison of the first diagonal velocities: numerical results with the exact solution for a two-dimensional free-surface flow

$\frac{x}{100} = \frac{y}{100}$	0	0·2	0·4	0·6	0·8	1	E_v
Exact	imposed	$0{\cdot}80 \times 10^{-2}$	0·064	0·218	0·512	imposed	
T3B	imposed	$0{\cdot}84302 \times 10^{-2}$	0·066376	0·22164	0·51393	imposed	0·30104
T6	imposed	$0{\cdot}8077 \times 10^{-2}$	0·064681	0·21772	0·51395	imposed	0·02062
T6B	imposed	$0{\cdot}80089 \times 10^{-2}$	0·064664	0·21774	0·51402	imposed	0·01874
T6BN	imposed	$0{\cdot}35206 \times 10^{-2}$	0·05566	0·20877	0·48797	imposed	0·27622
T6N	imposed		0·054135	0·21027	0·47854	imposed	0·26712

elements are obviously more accurate than the other elements and that the T3B element provides acceptable performance with less computational effort.

One-dimensional unsteady flow

Neglecting all non-linear terms in equations (1) and (2) and the surface level in equation (3) (with respect to the bottom depth), then the one-dimensional linear wave is governed by the following relations:

$$\frac{\partial u}{\partial t} + g\frac{\partial h}{\partial x} = 0,$$

$$\frac{\partial h}{\partial t} + \frac{\partial Hu}{\partial x} = 0.$$

Using the above two-dimensional finite element model, we study the propagation of the linear wave in a prismatic channel with a closed end (Figure 7). Considering the following boundary conditions:

$$u = 0 \quad \text{at} \quad x = x_0 \quad \text{and} \quad h = a\cos\omega t \quad \text{at} \quad x = L,$$

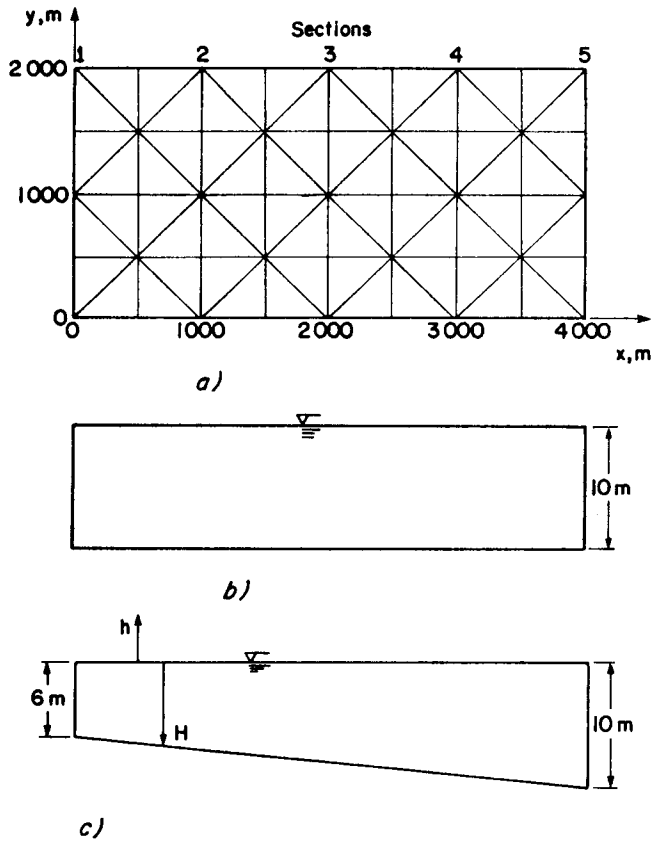

Figure 7. Mesh configuration of prismatic channel: (a) mesh configuration (b) constant depth $H = 10$ m; (c) variation of the depth H if the channel

and a constant bed slope, the exact solution is then determined analytically (cf. Appendix). A stable numerical solution has been obtained after three cycles of a period T of one hour, starting from rest, and with a time interval $\Delta t = 50$ s. Results are presented in Tables IV–VII. They are those for centre-line nodes where the two-dimensional flow is expected to behave unidirectionally.

Table IV. Comparison of numerical results and exact solution for the propagation of a linear wave: water levels at $t = 2{\cdot}0$, with $S_0 = 0$ and $\Delta t = 50$ s

Section	1	2	3	4	5
Exact	0·131	0·129	0·123	0·113	0·1
T3B	0·130	0·128	0·123	0·113	0·1
T6	0·130	0·128	0·122	0·113	0·1
T6B	0·130	0·128	0·123	0·113	0·1
T6BN	0·127	0·125	0·120	0·111	0·1
T6N	0·130	0·128	0·123	0·113	0·1

Table V. Comparison of numerical results and exact solution for the propagation of a linear wave: velocities at $t = 2{\cdot}25$ h with $S_0 = 0$ and $\Delta t = 50$ s

Section	1	2	3	4	5
Exact	0·000	0·023	0·045	0·066	0·084
T3B	0·0	0·0225	0·0442	0·0646	0·0798
T6	0·0	0·0224	0·0440	0·0645	0·0759
T6B	0·0	0·0225	0·0443	0·0645	0·0759
T6BN	0·0	0·0193	0·0380	0·0556	0·0698
T6N	0·0	0·0225	0·0443	0·0648	0·0850

Table VI. Comparison of numerical results and exact solution for the propagation of a linear wave: water levels at $t = 2{\cdot}0$, with $S_0 = 10^{-3}$ and $\Delta t = 50$ s

Section	1	2	3	4	5
Exact	0·1381	0·1349	0·1265	0·1145	0·1
T3B	0·1364	0·133	0·1254	0·1139	0·1
T6	0·1365	0·1334	0·1254	0·1139	0·1
T6B	0·1364	0·1335	0·1254	0·1139	0·1
T6BN	0·1322	0·1296	0·1226	0·1124	0·1
T6N	0·1354	0·1325	0·1246	0·113	0·1

Table VII. Comparison of numerical results and exact solution for the propagation of a linear wave: velocities at $t = 2.25$ h with $S_0 = 10^{-3}$ and $\Delta t = 50$ s

Section	1	2	3	4	5
Exact	0·0	0·0342	0·0585	0·0754	0·0866
T3B	0·0	0·0333	0·0572	0·0740	0·0834
T6	0·0	0·0322	0·0562	0·0730	0·0708
T6B	0·0	0·0322	0·5623	0·0730	0·0808
T6BN	0·0	0·0292	0·0504	0·0656	0·0749
T6N	0·0	0·0325	0·0563	0·0730	0·0814

The numerical results are satisfactory for all elements, considering the coarse mesh size used. An artificial diffusion introduces lateral velocities so that the flow is not strictly unidimensional. Less numerical diffusion has been observed with the T3B and T6BN elements. This diffusion is principally due to the time integrating scheme, which is known to be very dissipative.

In unsteady flows the consumption of computing time may constitute a strong constraint to be considered in practical applications. Simple elements such T3B and T6N could be efficient and competitive with the most popular T6 element. Indeed, in this simple example nearly 25 per cent of CPU time has been saved with those elements in comparison with the T6 element.

St. Lawrence River simulation

We have simulated the steady flow of the St. Lawrence River near the Gentilly area. The goal is to qualitatively compare the behaviour of the elements T6B, T6BN, T6N, T3B with the T6 element already used in Reference 21. The mesh used is presented in Figure 8. Surface levels are specified on open boundaries (the difference between the two levels is 0·20 m) and the no-slip condition has been applied to solid boundaries. From a practical point of view, the slip condition would have been preferable. However the present choice is made simply to eliminate the influence of boundary irregularities which vary for different types of elements, thus facilitating the comparison of results. Figure 9 presents an example of the velocity field obtained using the T3B element. Variations of the intensity of velocity and of the free surface level at sections A–A and B–B (see Figure 8) are presented in Figures 10 and 11. We conclude that:

1. The numerical results for the T6 and T6B elements are practically identical.
2. The difference between the T3B and T6 results has been observed to be less than 10 per cent for the velocity and less than 5 per cent for the water level. This is within the error associated with the model itself and can be considered as quite satisfactory. The greatest discrepancies correspond to the regions where the bathymetry varies rapidly, and thus for the simplest element (T3B) a local refinement of the mesh could be performed to improve the results. In term of time consumption the T3B element has offered a 45 per cent saving in time in comparison with the T6 element.
3. There is an appreciable discrepancy between results for the T6N element and the others.

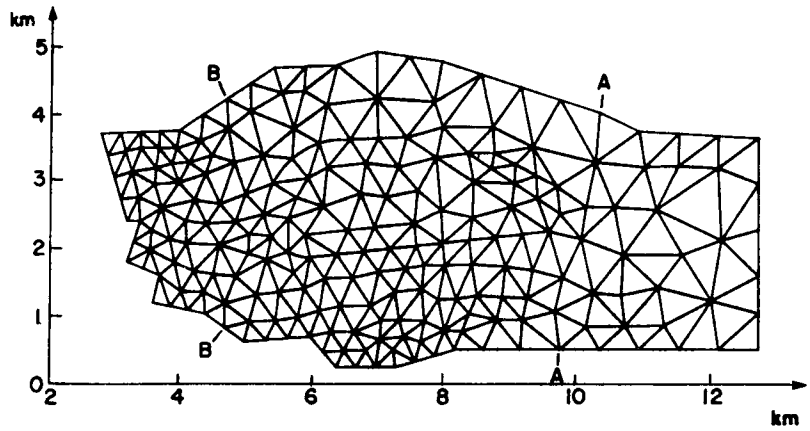

Figure 8. Gentilly: mesh configuration (374 elements)

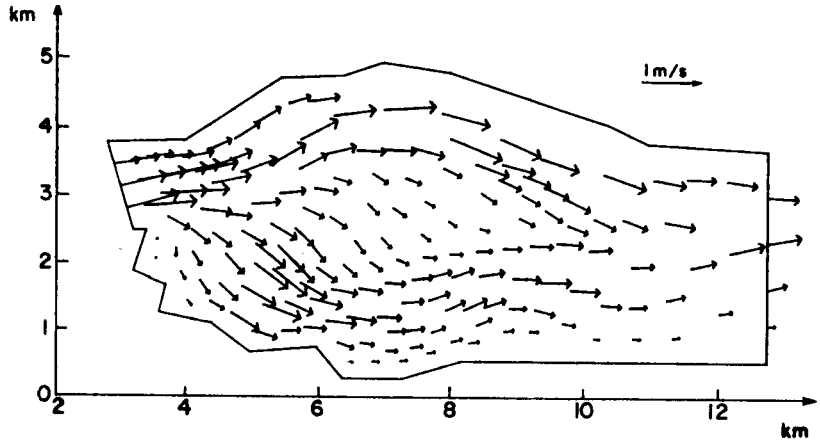

Figure 9. Gentilly: velocity field, steady flow

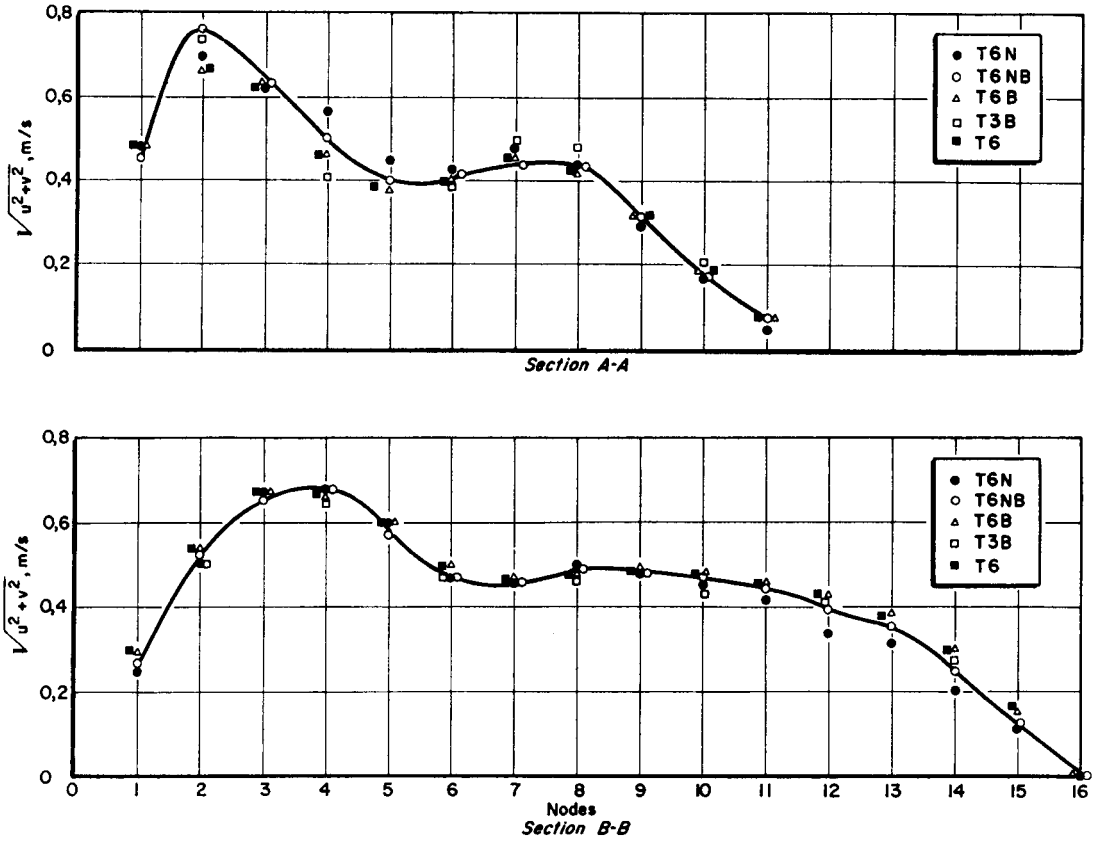

Figure 10. Gentilly: velocity distribution at sections A–A and B–B

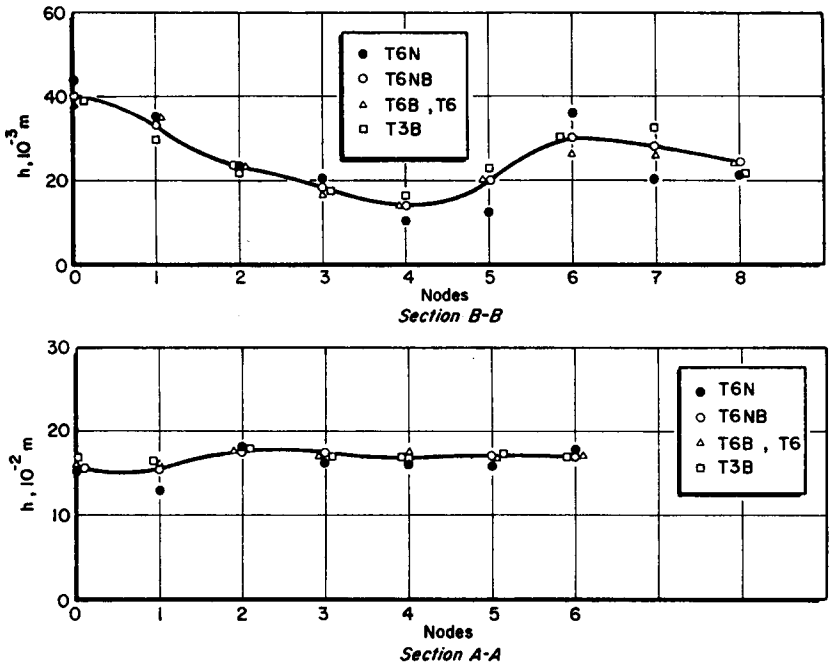

Figure 11. Gentilly: water level profile at sections A–A and B–B

Important oscillations of the free surface level have been observed and are shown in Figure 12. A chequerboard pattern is clearly present in these oscillation and this is a clear evidence of the instability of this element.

CONCLUSION

We have considered various bench-mark examples, some of them not classical, in order to assess the performance of the elements developed in this study. These examples may be useful to other researchers for making a preliminary evaluation of finite element codes. We consider, no doubt, the T6 element as the basis for comparison since it is employed most often in all practical studies. It seems that the simple T3B element offers excellent advantages in computational efficiency and simplicity for practical applications. We believe that this element could be easily integrated in a standard way in industrial codes for hydraulic flows. There is no evident advantage to using the T6B element. However the T6BN element effectively provides accuracy and efficiency between the most robust element T6 and the simplest element T3B. At present, we are trying to develop efficient elements for three-dimensional flows by extending the basic approximation techniques employed for the two-dimensional elements.

APPENDIX: PROPAGATION OF A LINEAR WAVE IN A CLOSED CHANNEL

When the non-linear terms of equations (1)–(3) are neglected for a one-dimensional flow, these reduce to the equations of the linear wave:

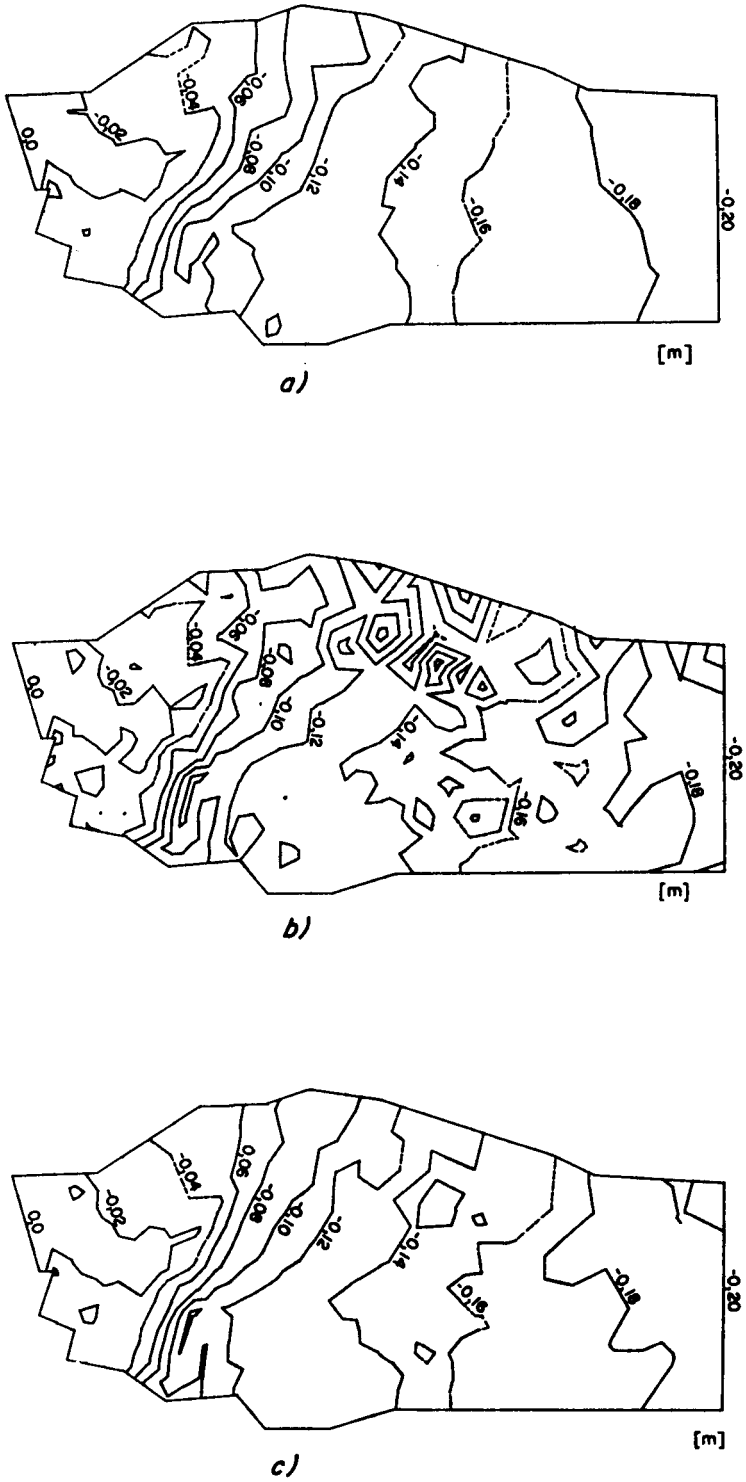

Figure 12. Lines of constant free surface elevation: (a) element T3B; (b) element T6N; (c) element T6

$$\frac{\partial u}{\partial t} + g\frac{\partial h}{\partial x} = 0,$$

$$\frac{\partial h}{\partial t} + \frac{\partial Hu}{\partial x} = 0.$$

We consider the following boundary conditions:

$$u = 0 \qquad \text{at} \quad x = x_0,$$
$$h = a\cos\omega t \quad \text{at} \quad x_1 = L + x_0.$$

In the case of a constant slope channel (S_0), the exact solution reads

$$h = [AJ_0(2\sqrt{(kx)}) + BY_0(2\sqrt{(kx)})]\cos\omega t,$$

$$u = \frac{g}{S_0 x}[AJ_1(2\sqrt{(kx)}) + BY_1(2\sqrt{(kx)})]\sin\omega t,$$

where

$$A = \frac{a}{D}Y_1(2\sqrt{(kx_0)}),$$

$$B = \frac{a}{D}J_1(2\sqrt{(kx_0)}),$$

$$D = Y_1(2\sqrt{(kx_0)})J_0(2\sqrt{(kx_1)}) - Y_0(2\sqrt{(kx_1)})J_1(2\sqrt{(kx_0)}).$$

J and Y are the Bessel functions of first and second orders, x_0 is the position of the inlet boundary, x_1 is the position of the outlet boundary, L is the length of the channel, ω is the angular frequency, $k = \omega^2/S_0 g$ is the wave number, $c = \sqrt{(gH)}$ is the celerity of the wave and H is the depth of the basin.

REFERENCES

1. D. W. Pritchard, 'Estuarine modelling an assessment', in G. H. Ward and W. H. Epsey (eds), *Nat. Tech. Inf. Ser.*, 1971, pp. 206–807.
2. J. J. Leenderste, 'Aspects of a computational model for long period water-wave propagation', *Ph.D. Thesis*, Delft, 1967.
3. C. Taylor and P. Hood, 'Numerical solution of the Navier–Stokes equations using the finite element technique', *Comp. and Fluids*, **1**, 1–28 (1973).
4. J. J. Connor and J. D. Wang, 'Finite element modelling of hydrodynamic circulation', in C. A. Brebbia and J. J. Connor (eds), *Num. Math. in Fluid Dynamics*, Pentech Press, 1974.
5. F. Brezzi, 'On the existence, uniqueness and approximation of saddle point problems arising from Lagrange multipliers', *R.A.I.R.O., Série Rouge*, **R2**, 123–151 (1974).
6. I. Babuska, 'Error bounds for finite element method', *Num. Math.*, **16**, 322–333 (1971).
7. R. L. Sani, P. M. Gresho, R. L. Lee and D. F. Griffiths, 'The cause and cure of the spurious pressures generated by certain F.E.M. solutions of the incompressible Navier–Stokes equations', *Int. j. numer. methods fluids*, **1**, 17–43 and 171–204 (1981).
8. M. Fortin, 'Old and new finite element method for incompressible flows', *Int. j. numer. methods fluids*, **1**, 347–364 (1981).
9. J. T. Oden and G. F. Carey, *Finite Elements, Mathematical Aspects*, Volume IV, Prentice-Hall, 1983.
10. V. Girault and P. A. Raviart, 'Finite element approximation of the Navier–Stokes equations', *Lecture notes in Mathematics, no. 749*, Springer-Verlag, 1981.
11. J. F. Cochet, 'Modélisation d'écoulements stationnaires et non stationnaires par éléments finis', *Thèse de Docteur ingénieur*, Université de technologie de Compiègne, 1979.
12. J. F. Cochet, G. Dhatt and G. Touzot, 'Comparison of explicit and implicit methods applied to finite element models of tidal problems', *3rd Int. Conf. on F.E. in Flow Problems*, Banff, 1980.
13. R. A. Walters and R. T. Cheng, 'Accuracy of an estuaries hydrodynamical model using smooth elements', *Water Resources Research*, **16**, (1), 187–195 (1980).

14. D. N. Arnold, F. Brezzi and M. Fortin, 'A stable finite elements for the Stokes equations' (to appear in *Calcolo*).
15. A. Soulaimani, 'Nouveaux aspects de l'application de la méthode des éléments finis en hydrodynamique', *M.Sc. Thesis*, Laval University, 1983.
16. A. Fortin, 'Méthodes d'éléments finis pour les équations de Navier–Stokes', *Ph.D. Thesis*, Laval University, Québec, 1984.
17. M. Bercovier and O. Pironneau, 'Error estimates for finite element method solution of the Stokes problem in primitive variables', *Lecture notes in Mathematics*, Springer-Verlag, 1976, pp. 211–224.
18. A. Fortin and M. Fortin, 'Newer and newer elements for incompressible flow', in R. H. Gallagher, G. Carey, J. T. Oden and O. C. Zienkiewicz (eds), *Finite Elements in Fluids, Volume 6*, Wiley, Chichester, 1986.
19. G. Dhatt and G. Touzot, *The Finite Element Method Displayed*, Wiley, 1984.
20. Michel Fortin *et al.*, 'Simple continuous elements for incompressible flows', (in preparation).
21. J. F. Cochet, G. Dhatt, G. Hubert, Y. Ouellet, J. L. Robert and J. L. Verrette, 'Gentilly-3—Modélisation et mécanismes de rejet d'eau de refroidissement', *Rapport CRE-83-01*, Centre de recherches sur l'eau, Université Laval, Québec, 1983.